이학석사학위논문

과산화수소와 글루코오스 검출을 위한 BODIPY 기반의 전기화학발광 프로브

BODIPY-Based Electrochemiluminescent Probes for Rapid Detection of H_2O_2 and Glucose

2019 년 8 월

서울대학교 대학원

화학부 유기화학 전공

남 궁 연

Abstract

BODIPY-Based Electrochemiluminescent Probes for Rapid Detection of H_2O_2 and Glucose

Yon Namkoong

Major in Organic Chemistry

Department of Chemistry

Graduate School

Seoul National University

Electrochemiluminescence (ECL) is a powerful analytical tool for point-of-care testing (POCT) of diagnostic biomarkers. Organic ECL emitters based on boron-dipyrromethene (BODIPY) have been developed but rarely applied to small-molecule detection. Herein, we report three BODIPY-based probes for detection of hydrogen peroxide (H_2O_2), one of the reactive oxygen species, and glucose which is the typical sign of various diseases such as diabetes. The diethyl-introduced probes exhibited enhanced ECL intensity in response to H_2O_2, which improved the sensitivity of detection. Moreover, fluorination near the recognition site, boronate

pinacol ester, accelerated the detection speed. Our ECL probe **2F** proved to be effective by the sensitive and selective detection, indicating the potential application into POCT. The applicability of **2F** was further assured by the real sample experiment in which glucose present in human serum was precisely quantified.

Keywords: Electrochemiluminescence (ECL) Probe, BODIPY, hydrogen peroxide, Glucose, Glucose oxidase, Real-sample detection.

Student Number: 2017–21746

Contents

A. Background

A.1. Electrochemiluminescence (ECL)[1]

A.1.1. Fundamentals of ECL

Electrochemiluminescence or electrogenerated chemiluminescence (ECL) is a light-emitting process by the formation of an excited state *via* an electron transfer between radical species produced when electric potential is given. ECL analysis offers several advantages compared to photoluminescence. Firstly, no expensive instrumentation is needed for excitation. As ECL is generated with electrode, its instrumentation and instruction are especially simple compared to other optical techniques. The simplified set-up enables its application for point-of-care testing (POCT) and field-monitoring.[2] Small interference and high sensitivity are also the strengths that ECL has.[3] High sensitivity and wide linear range are well-known advantages that make ECL a powerful analytical method. ECL has found a variety of applications in immunoassays and DNA analyses by employing ECL-active species as labels on biomolecules.[4] Its application into small-molecule detection has obtained huge interest because of high sensitivity and selectivity.[5]

A.1.2. Annihilation ECL

In annihilation pathway, which is the most fundamental method, both the radical cation and radical anion of luminophore are generated by the potential sweep of a working electrode from negative to positive range.[6,7] Then, electron transfer between them forms an excited state that can realize luminescence. The general annihilation mechanism is outlined below:

$$A - e^- \rightarrow A^{\bullet +}$$

$A + e^- \rightarrow A^{\bullet -}$

$A^{\bullet -} + A^{\bullet +} \rightarrow A^{\bullet} + A$

$A^{\bullet} \rightarrow A + h\nu$

A indicates a luminophore such as $Ru(bpy)_3^{2+}$, for instance. ECL is generated when a double potential step is applied to an electrode such as glassy carbon, producing the radical cation, $A^{\bullet +}$ upon anodic oxidation and the radical anion, $A^{\bullet -}$, upon cathodic reduction. The resulting electrogenerated products can react and undergo annihilation to produce an excited state, $A^{\bullet}$, which is able to emit light.

The annihilation approach begins with an alternate pulsing of the electrode potential. Thus, the wide potential window of the solvents is required, which excludes all the aqueous solvents. Also, both the oxidized and reduced radical species should be stable.

A.1.3. Coreactant ECL[8]

Coreactants are species producing an intermediate that helps ECL luminophore to form its excited state. Most annihilation systems require the high purity of solvents to avoid the disruption caused by oxygen or water contents in samples. On the other hand, a coreactant allows to generate potential sweep in one direction only and therefore, it is possible to overcome the narrow potential window of some solvents, especially water, and formation of unstable radical ions of luminophore. There are two kinds of ECL coreactants: oxidative-reductant and reductive oxidant. Oxidative-reductive coreactants such as oxalate ($C_2O_4^{2-}$) are often used for reduction ECL, which produces the strong reductant $CO_2^{\bullet -}$ upon oxidation. the excited state is generated by an electron transfer between $CO_2^{\bullet -}$ and radical anion of luminophore. Tri-*n*-propylamine (TPrA) is often referred as the latter type of coreactants with

strong oxidizing ability and the optimum ECL among the other amine-based coreactants. The ECL mechanism in the presence of TPrA is depicted in scheme 1 and followed below:

$$TPrA - e^- \rightarrow TPrA^{\bullet+} \rightarrow TPrA^{\bullet} + H^+$$

$$A - e^- \rightarrow A^{\bullet+}$$

$$TPrA^{\bullet} + A^{\bullet+} \rightarrow A^{\bullet} + \text{byproduct}$$

$$A^{\bullet} \rightarrow A + h\nu$$

Notice that the radical anion of luminophore ($A^{\bullet-}$) is not formed in this mechanism.

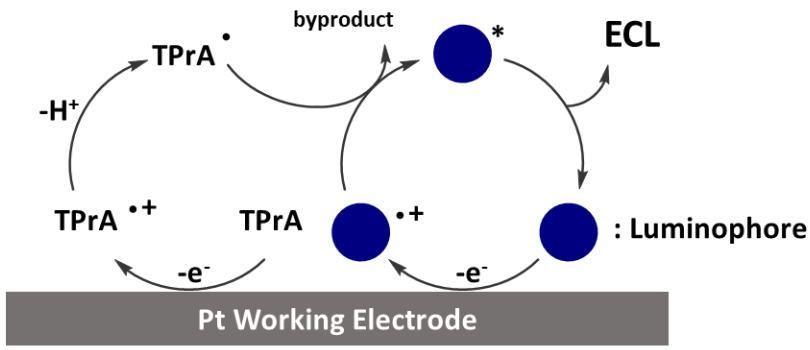

Scheme 1. ECL mechanism in TPrA coreactant system

A.2. ECL Luminophores

A.2.1. General ECL luminophores

There are three types of ECL luminophore: inorganic, organic, and nanomaterials. Most recent studies mainly utilized metal complexes, luminol, and nanocomposites. Metal complexes are extensively studied for three main reasons. Firstly, tris (2,20 - bipyridine) ruthenium (II) ($Ru(bpy)_3^{2+}$) ECL has exhibited overwhelming ECL

performances due to its high sensitivity, wide dynamic range, and stable labels.[9] Secondly, a direct detection of numerous analytes by metal complexes leads to its broad applications.[10] Lastly, the color tunability is significant in metal complexes, particularly in ruthenium complex ECL. In comparison to the molecular luminophore, nanomaterials, such as nanocrystals, nanoclusters, carbon nanocomposites, have been demonstrated recently owing to their versatility and fine properties.[8]

Among them, organic ECL emitters have several superiorities in terms of their cost-effective synthesis and easy structural modulation for regulating energy level or water solubility aside their good biocompatibility.[11] The early studies for organic ECL involved polycyclic aromatic hydrocarbons such as anthracene and rubrene. However, their poor solubility in water hindered them from practical application.[6] Luminol ECL also has gained some popularity mainly from its low cost, easy functionalization, and broad bio-applications, as similar to organic molecular luminophores. However, using luminol has a serious drawback for a bioanalytical application that it works usually in highly basic condition, over pH 9.[12]

A.2.2. ECL of BODIPY dyes[13]

Recently, non-polyaromatic hydrocarbons such as perylene diimide, fluorescein, and boron-dipyrromethene (BODIPY) have been studied. Especially, many researches about electrochemistry and ECL of BODIPY dyes have been conducted and proved that completely substituted BODIPY dyes produce stable and intense ECL signals. However, their application for small molecule detection still remains a challenge. To our best knowledge, there has been no report of BODIPY-based ECL sensor since our group developed a pyrophosphate receptor.

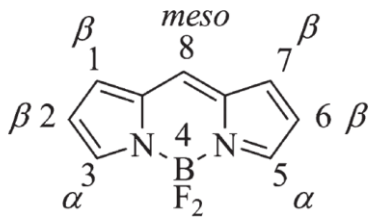

Scheme 2. Structure of BODIPY

The electrochemical properties of BODIPY derivates strongly depend on the substitution in the dye core (Scheme 2). While a completely substituted dye shows reversible Nernstian reduction and oxidation, the absence of substitutes in position 2, 3, 5, and 6 causes the formation of unstable radical cation, and anion in case of position 8. The steric protection on the BODIPY core prevents the dimerization and polymerization similar to the behaviors of pyrroles.

A.3. ECL Probes

Based on a variety of molecules that exhibit ECL, a lot of publications concerned with analytical applications of ECL are published. It is one way to utilize ECL active

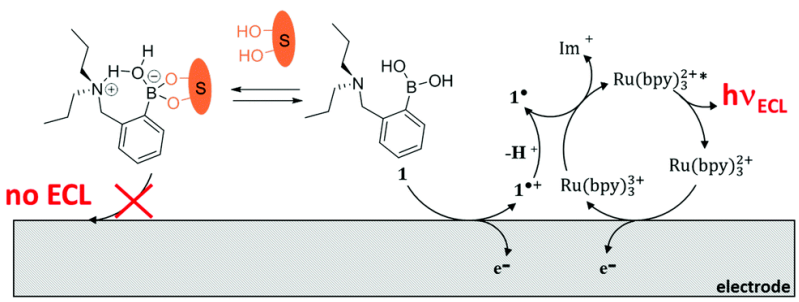

Figure 1. Influence of the binding equilibrium of phenylboronic acid to the saccharides (either D-fructose or D-glucose) on the ECL mechanism of the system $Ru(bpy)_3^{2+}$/**E0**. Im+ is the iminium product.

compounds as a signaling unit and attach a reaction unit to it, and another could be to introduce a recognition unit of the target analyte at the ECL coreactant. The report of a strategy for modulating the ECL response by integrating a boronic acid to the chemical structure of coreactants showed excellent selectivity for D-glucose by tuning the linker length of a bis-boronic acid amine coreactant (Figure 1).[14]

The more conventional method is to exploit an ECL luminophore as a molecular sensor. Our group has been developing ECL chemosensors based on cyclometalated Ir(III) complex. To date, the most of ECL probes have been based on ruthenium complexes because of their well-defined properties, good solubilities and high ECL efficiencies. However, we reported a series of ECL probes based on Ir(III) complexes that exhibits the overwhelming properties greater than Ru(II) derivatives. Our latest publication reported a highly sensitive ECL turn-on chemodosimeter based on cyclometalated Ir(III) complexes for thiophenol detection.[15]

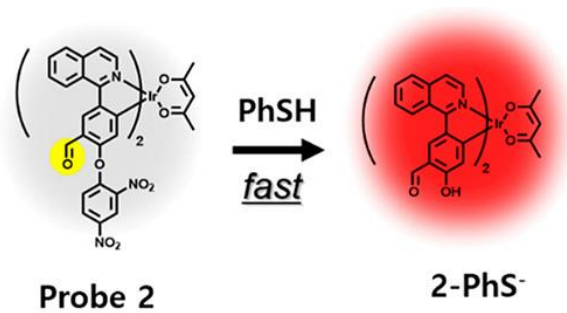

Figure 2. Design of an ECL probe based on cyclometalated Ir(III) complex for rapid detection of thiophenol.[15]

A.4. Research Purposes

Our research aims to develop an efficient ECL probe by utilizing BODIPY dyes as a signal unit. We introduced a boronate pinacol ester group for determination of hydrogen peroxide and glucose in aid of the enzymatic detection method. Once the high sensitivity and selectivity of probe are provided, quantification of glucose in real sample such as blood or urine was conducted to demonstrate the potential application of the BODIPY-based ECL probe for point-of-care testing.

B. BODIPY-Based Electrochemiluminescent Probes for Rapid Detection of H_2O_2 and Glucose

B.1. Introduction

Electrochemiluminescence (ECL) proved to be powerful in analytical applications due to its combined advantages from chemiluminescence and electrochemistry.[1,3,8] Like other chemiluminescent analyses, ECL is generated as a result of electrochemical reactions but on electrode surface when electric potential is applied.[9,10,16] Thus, low background signal is the distinctive feature that enables improved analytical sensitivity.[8,17] The other notable advantage of ECL over other optical sensing techniques is that no external light source is necessary.[5] By eliminating the light source, the instrument setup could be much simpler and more versatile in the development of portable point-of-care testing (POCT) devices for medical diagnostics.[2,8] Moreover, ECL was applied as an alternative surface-confined microscopy to imaging single cells and their membrane proteins.[18]

Organic ECL emitters have several advantages compared to inorganic materials in terms of their cost-effective synthesis, easy structural modulation for regulating energy levels or water solubility, and their good biocompatibility.[8,11] Among various organic ECL compounds, boron-dipyrromethene (BODIPY) dyes have received much attention for their exceptionally high brightness[19,20] and thus have been exploited as a variety of photoluminescent (PL) probes.[21,22] When combined with ECL, BODIPY derivatives can exhibit further improved sensing ability considering their typical small Stokes shift[23-25] which can be included in the background noise in PL detection. Hence, electrochemistry and ECL of BODIPY

derivatives have been studied extensively by Bard and co-workers,[13] but their application for small molecule detection still remains a challenge.[26]

Hydrogen peroxide (H_2O_2) is an important reactive oxygen species (ROS) involved in a number of physiological and pathological processes as an oxidant and a signaling molecule in the human body.[24,27] It has been known that abnormally high concentrations of H_2O_2 can cause serious oxidative damage to cellular components and associate with various diseases such as cancer, cardiovascular diseases, and neurological disorders.[27,28] Therefore, selective and sensitive detection of H_2O_2 is of great importance.

As H_2O_2 is involved in many enzyme-catalyzed reactions and generated as their side-product, monitoring H_2O_2 can determine substrates of enzymes such as horseradish peroxidase, superoxide dismutase, and catalase.[29] Thus, H_2O_2 probes can determine glucose when coupled with glucose oxidase (GOx), known to selectively oxidize glucose releasing H_2O_2 and gluconic acid,[30] Glucose is a meaningful target for ECL probes as its detection can be utilized in POCT of blood glucose levels, which are the obvious mark of hyperglycemia[31,32] and diabetes.[33]

Boronate pinacol ester (Bpin) is known for its specific oxidation by H_2O_2 at mild pH conditions and unique fluorescence quenching behavior due to the electron accepting ability resulting in turn-on luminescence of probe in response to the analyte.[34-38] Thus, a Bpin moiety was attached to our probe as a reaction unit in regards to guaranteed selectivity and sensitivity. However, most of Bpin-containing probes generally complete the detection in 1-2 h at room temperature.[39-41] To maximize the most important advantage of ECL that is applicable for POCT, the detection time should be reduced. We devised simple fluorination near the reaction unit to lower its pK_a by the electron-withdrawing effect of fluorine.[36,42]

Herein, we report BODIPY-based ECL probes (**1**, **2**, **2F**) for H_2O_2, among which **2F** successfully detects H_2O_2 in 30 minutes at room temperature. Considering its improved ECL properties and detection speed, we suggest probe **2F** as a facile indicator of H_2O_2 and glucose that can successfully work at the point of need. Furthermore, the potential application of probe **2F** is highly promising in real sample detection as demonstrated in determination of the serum glucose level.

B.2. Results and Discussion

B.2.1. Design and Synthesis

Our aim was to develop an effective ECL probe for H_2O_2 based on BODIPY dyes. The design concept of our probes are described in Scheme 1a. Probe **1** consists of pyridine-extended BODIPY (**py1**) and Bpin connected with a benzyl moiety, which is a typical self-immolative linker.[43] The action of H_2O_2 converts the boronate into the corresponding hydroxyl group, followed by a spontaneous release of a bright fluorescent product (**py1**). Considering the high quantum efficiency of most BODIPY derivatives, high turn-on ratio of the probe is expected upon reaction with analytes.

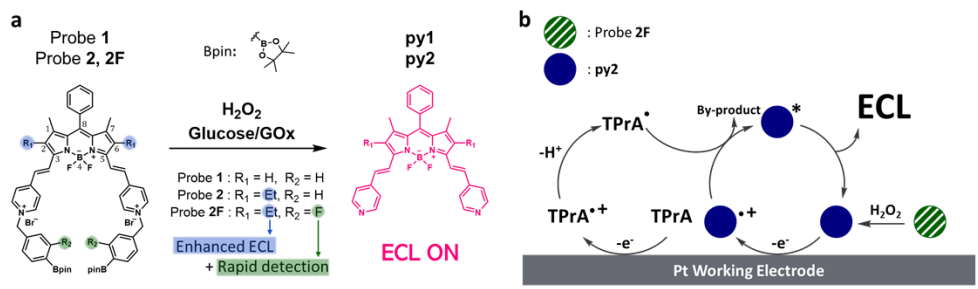

Scheme 3. Design concept of probes and (b) proposed ECL sensing mechanism of H_2O_2 by probe **2F** in the TPrA co-reactant pathway.

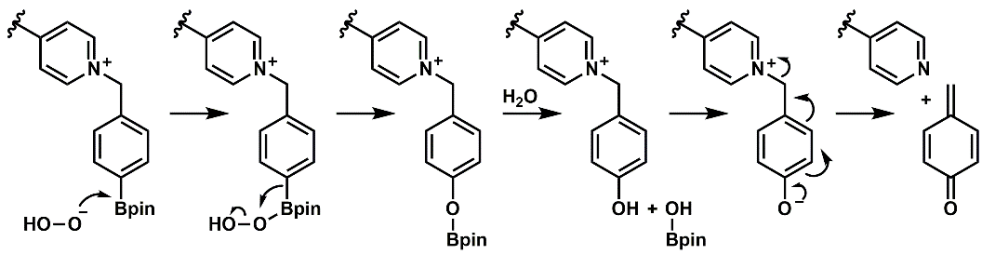

Scheme 4. Proposed Mechanism of the Reaction Unit in Response to H_2O_2.

The sound operation of an ECL sensor requires its molecular stability, as well, as a variety of radical species take part in the ECL process. As shown in Scheme 1b, the positive potential at the working electrode oxidizes the luminophore, **py2**, and the co-reactant, tri-*n*-propylamine (TPrA), producing their radical cations, **py2**$^{\bullet+}$ and TPrA$^{\bullet+}$. Then, by the electron transfer from deprotonated TPrA radical (TPrA$^{\bullet}$) to **py2**$^{\bullet+}$, the excited state **py2*** is formed that can release ECL. Thus, the stability of the radical cation of probes is essential in the TPrA co-reactant pathway, otherwise undesirable side-reactions such as dimerization can disturb the process. In case of BODIPY dyes, the stability of their radical cations strongly depends on the substitution at the positions 2 and 6 of BODIPY (Scheme 3a).[13] Therefore, two ethyl

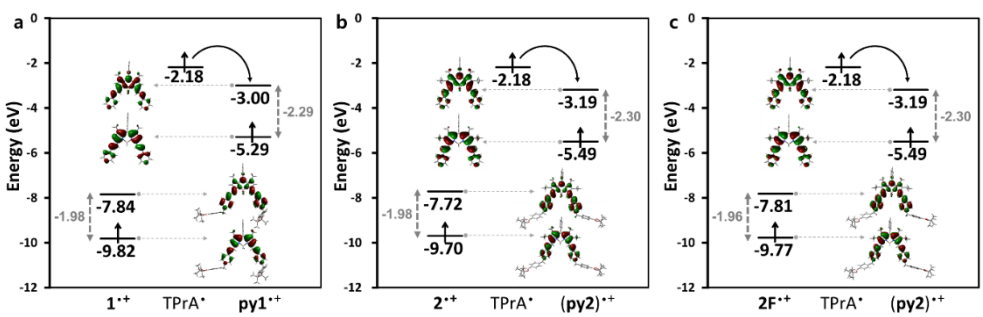

Figure 3. DFT calculations (by Gaussian '09, B3LYP/6-31G level) of HOMO and LUMO energy levels of radical species generated during the ECL process for probe **1** (a), **2** (b), and **2F** (c) before and after reaction with hydrogen peroxide in presence of TPrA as a co-reactant.

groups were introduced into the 2,6-positions of probe **1** (probe **2**) to improve electrochemical stability.

Moreover, the short operation time will maximize the benefits of POCT application. As described in Scheme 4, the suggested reaction mechanism includes pH-dependent steps which could be accelerated by lowering pK_a of the reaction unit, phenyl Bpin group. The corresponding phenol intermediates are generated during the reaction with H_2O_2. After comparing the pK_a values of *ortho*- and *meta*-fluorophenol, 8.73 and 9.28,[44] respectively, we introduced fluorine at the *ortho*-site of the phenyl Bpin (**2F**) to assist deprotonation of the phenol intermediate. **2F** emits light from the same product **py2** that probe **2** releases upon reaction with H_2O_2 but is expected to have enhanced detection speed.

The energy levels of three probes were estimated by density function theory (DFT) calculations to ensure that the electron transfer easily occurs between $TPrA^{\bullet+}$ and the radical cation of the probes (Figure 3) and later experimentally demonstrated

Table 1. Electrochemical properties and HOMO/LUMO energy levels of probes

	E_{ox} [a] (V vs. Fc/Fc$^+$)	HOMO (eV)[b]	LUMO (eV) [c]	$E_{g,op}$ (eV) [d]	$E_{g,cal}$ (eV) [e]
Probe **1**	0.89, 1.32	-5.69	-3.84	1.85	1.98
Probe **2**	0.88, 1.30	-5.68	-3.88	1.80	1.98
Probe **2F**	0.84, 1.38	-5.64	-3.81	1.83	1.96
py1	1.01	-5.81	-3.79	2.02	2.29
py2	1.04	-5.84	-3.88	1.96	2.30

[a] The onset oxidation potential determined by CV.

[b] HOMO levels calculated by the following equation: HOMO (eV) = – (E_{ox} – $E_{Fc/Fc+}$) – 4.80

[c] LUMO estimated using the optical band gap ($E_{g,op}$)[d]

[e] E_g calculated by DFT calculation.

by cyclic voltammetry (CV) (Table 1). Probes **1**, **2**, and **2F** were synthesized as shown in Scheme 5. The BODIPY cores were prepared as reported[20] and then subjected to the microwave-assisted Knoevenagel condensation with pyridine-4-carboxaldehyde to give **py1** and **py2**. Finally, *N*-benzylation with bromomethyl phenyl boronate pinacol esters resulted in probes **1**, **2**, and **2F** *via* the S_N2 reaction. All new compounds were characterized by ^1H, ^{13}C NMR, and HRMS which are detailed in the supporting information.

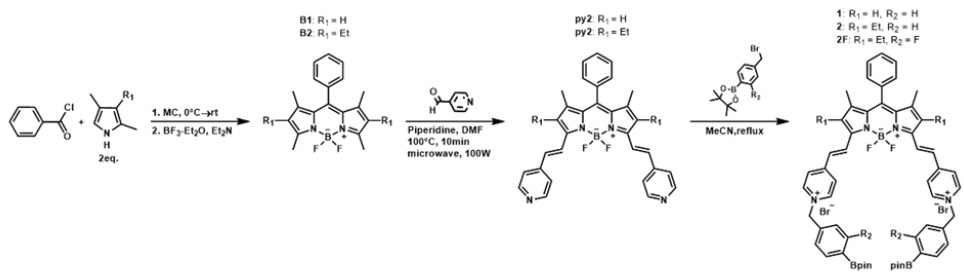

Scheme 5. The Synthetic Procedure of Probe **1**, **2**, and **2F**.

B.2.2. H_2O_2 Response of Probes

Examining photophysical properties of probe **1** in various conditions, the best environment was settled for effective detection of H_2O_2. The responses of probes toward H_2O_2 were assessed in 1:1 (v/v) mixture of acetonitrile and phosphate buffer (50 mM, pH 8). The reactions of probe **1** with H_2O_2 were saturated within 1 h at room temperature. For excellent sensing performances in ECL system, ECL intensities were measured in a voltage range from -0.1 V to 1.9 V at a scan rate of 1.0 V/s (Figure 4).

UV-vis absorption and fluorescence emission were evaluated before and after reaction with H_2O_2 (Figure 5a-f). Probes **1**, **2**, and **2F** showed strong absorption at 655, 670, and 665 nm, respectively, but their emission was effectively quenched

by Bpin. Upon addition of H_2O_2, the maximum absorption peaks were slightly red-shifted, resulting in the color change from green to purple which is detectable with naked eyes. The fluorescence changes were more prominent as bright red fluorescence was significantly turned on at 625 nm (**1**, 29-fold) and 640 nm (**2**, 66-fold; **2F**, 31-fold). While all probes displayed similar behavior in absorption and emission measurements, the ECL response of **1** was significantly distinguished from those of **2** and **2F**. As depicted in Figure 5g-i, the ECL signal of **1** is much lower than those of **2** and **2F** in response to H_2O_2, only reaching less than a quarter of the maximum intensity of **2F**. Therefore, **2** and **2F** represent suitable ECL probes for H_2O_2.

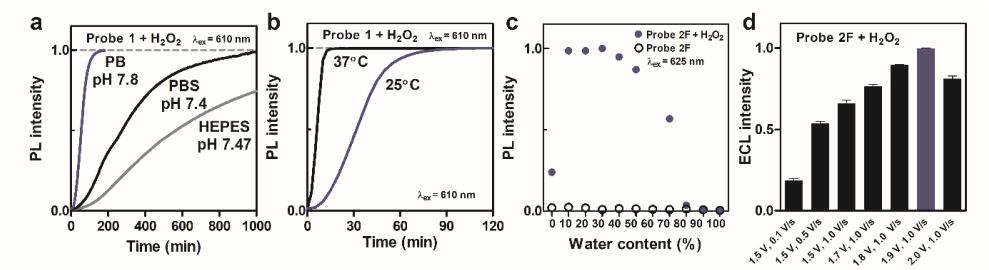

Figure 4. Optimization of PL and ECL experimental conditions: (a) Normalized PL intensity change of probe **1** at 625 nm with H_2O_2 in different buffer solutions, and (b) temperatures; (c) Relative PL intensity at 640 nm of probe **2F** before and after reaction with H_2O_2 in different water contents. (d) ECL dependence on applied potential and scan rate in the presence of 0.1 M TBAP and 67.5 mM TPrA. The experiments were conducted with 10 μM probe and 200 μM H_2O_2 in 1:1 (v/v) mixture of acetonitrile and 50 mM phosphate buffer (pH 8) at 25℃.

The oxidation of the phenyl Bpin moiety by H_2O_2 was monitored by ^1H NMR analysis. We synthesized model compounds **M** and **MF** imitating the reaction part of probes **2** and **2F**, respectively. The reaction of **M** with 5 equivalent H_2O_2 was recorded each hour in D_2O (5% DMSO-d_6) and partial signals of collected spectra are described in Figure 6. The oxidation of the C-B bond was completed 8 h after the addition of H_2O_2, as indicated by the upfield chemical shift changes of phenyl protons from 7.85 (H6), 7.49 (H5) to 6.99 (H6‘), 7.41 ppm (H5‘), respectively

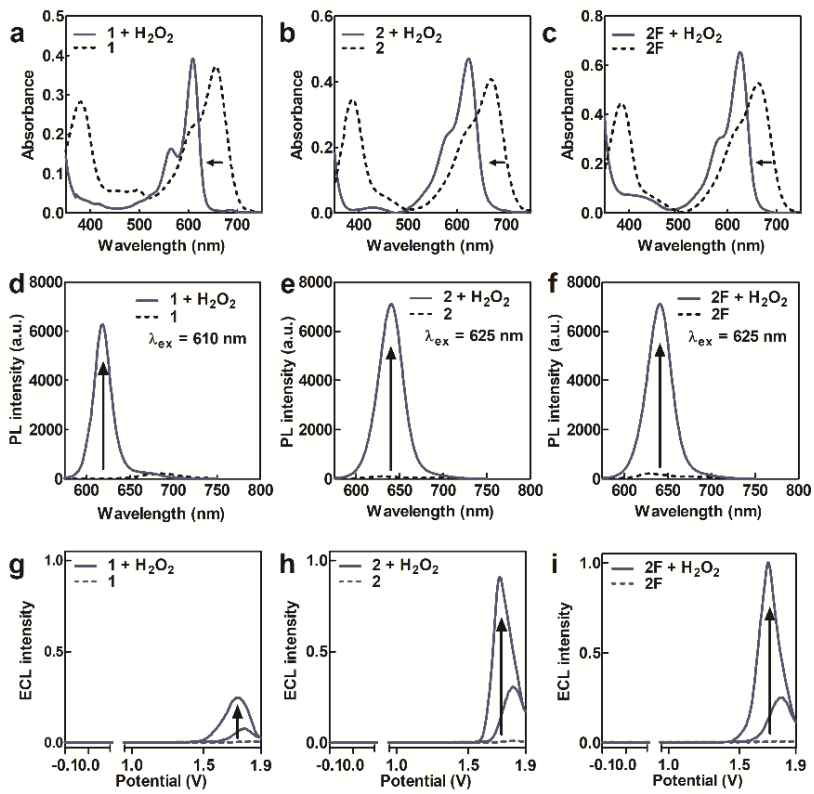

Figure 5. Absorption (a-c), emission spectra (d-f), and ECL responses of 10 μM probe **1** (a, d, g), **2** (b, e, h), and **2F** (c, f, i) after 30 min (probe **2F**) or 1 h (probes **1**, **2**) incubation with 200 μM H_2O_2 at 25℃ in a 1:1 (v/v) mixture of acetonitrile and potassium phosphate buffer (50 mM, pH 8.0).

(Figure 6b). As soon as 5 equivalent NaOH was added, all the aromatic peaks of **M** were upshifted, indicating that the borate intermediate was activated by the base component (Figure 6c). After 24 h, the peaks of the intermediate (Figure 6c) totally disappeared and there observed the resonances of 4- methyl pyridine at 7.35 (H2‘‘‘) and 8.41 ppm (H3‘‘‘), and quinone methide at 6.64 (H6“‘) and 7.17 (H5‘‘‘) ppm (Figure 6d). The full spectra of ^{1}H NMR analysis of **M** and **MF** are described in Figure 7.

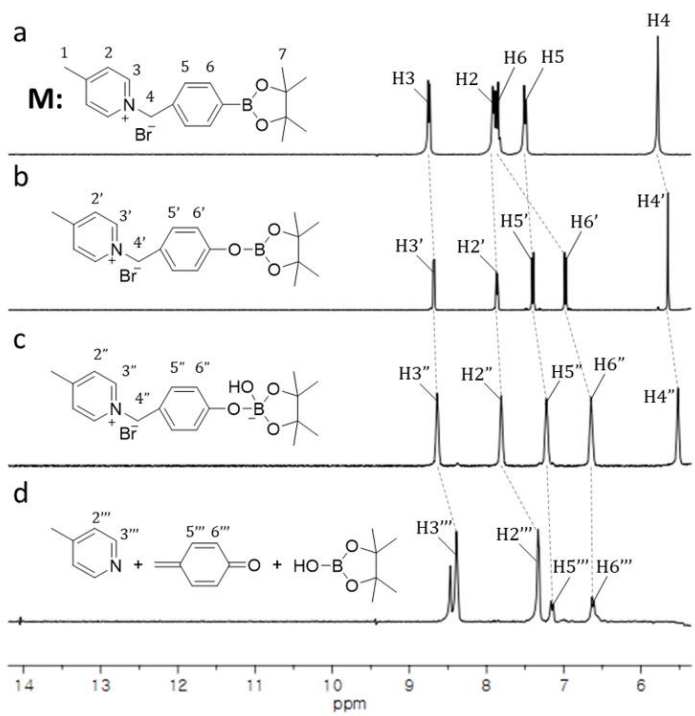

Figure 6. ^{1}H NMR analysis of the reaction of 15 mM **M** with 75 mM H_2O_2 in D_2O (5% DMSO-d_6); (a) before and (b) 8 h after the addition of H_2O_2, (c) 5 min and (d) 24 h after the addition of 50 mM NaOH to the solution of (b). NMR peaks of the observed.

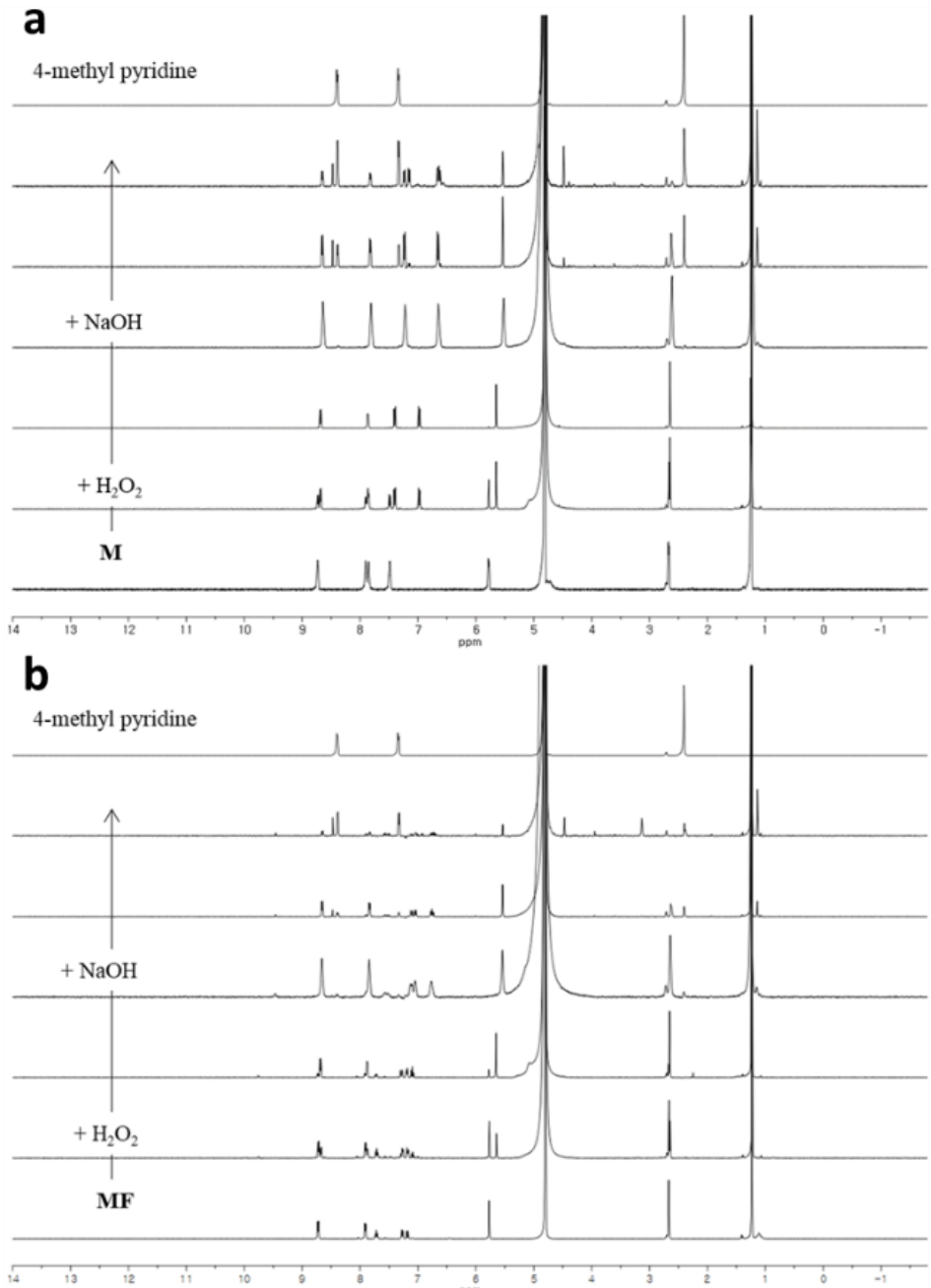

Figure 7. ^{1}H NMR analysis of 15 mM **M** (a) and **MF** (b) in response to H_2O_2 (150 mM) in D_2O (5% DMSO-d_6).

B.2.3. Enhancement of Detection Speed by Fluorination

The fluorescence intensities of **2** and **2F** were measured every 30 minutes after the addition of H_2O_2 in the pH ranges of 5.0 to 9.0 (Figure 8a-b). Both probes showed no change in fluorescence at mild acidic conditions because the reaction proceeds by nucleophilic addition of H_2O_2. In mild basic pH environments (pH 7.0, 7.4, 7.8, 8.0, 9.0), the fluorescence increases of probes **2** and **2F** at 640 nm were recorded (Figure 8c) and their maximum velocity (v_{max}) and 90% saturation time ($t_{0.9}$) were calculated in Table 2. It is noticeable that all v_{max} values of **2F** exceeded those of **2**. At the optimized pH condition, pH 8.0, the fluorescence of probe **2** reached its 90% saturation point 58 minutes after addition of 20 equivalent H_2O_2 while probe **2F** required 32 min only. Considering that most of the reported H_2O_2 probes with Bpin groups detected their target molecule in 1–2 h,[39-41] the detection speed of **2F** clearly stands out.

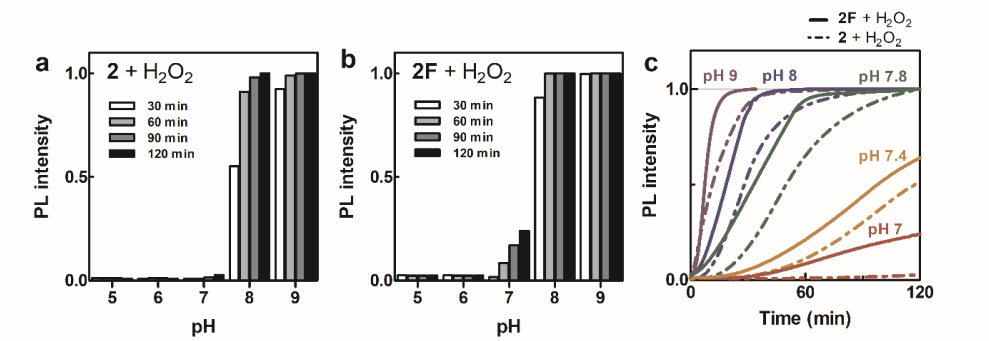

Figure 8. Normalized PL intensity at 640 nm of 10 μM probes **2** (a) and **2F** (b) with 200 μM H_2O_2 measured every 30 min for 2 h at various pH (5.0 – 9.0) in 1:1(v/v) mixture of acetonitrile and citrate/potassium phosphate buffer (50 mM) at 25℃. (c) Normalized PL intensity change at 640 nm of probes **2** and **2F** in response to 200 μM H_2O_2 in the physiological pH region (pH 7.0 – 9.0) (λ_{ex} = 625 nm) in 1:1(v/v) mixture of acetonitrile and potassium phosphate buffer (50 mM) at 25℃.

Table 2. Enhancement of the detection rate by fluorination.

	v_{max} (10^{-2}·min^{-1}) at 25℃ [a]				$t_{0.9}$ (min) [b]
	pH 7.4	pH 7.8	pH 8.0	pH 9.0	at pH 8.0, 25℃
Probe **2**	0.807	1.83	2.96	5.06	58
Probe **2F**	0.839	1.87	3.92	12.0	32

[a] The maximum velocity of each reaction calculated by differentiation of time-dependent PL intensity changes (Figure 8c, OriginPro 8). [b] 90% saturation time when the fluorescence intensity reaches 90% of its maximum.

B.2.4. ECL Sensitivity and Selectivity

ECL experiments were performed to investigate the sensitivity and selectivity of **2F** toward H_2O_2 (see Figure 9 for the PL performances of **2F** toward various analytes). As shown in Figure 10a, the ECL intensities significantly increased with gradually

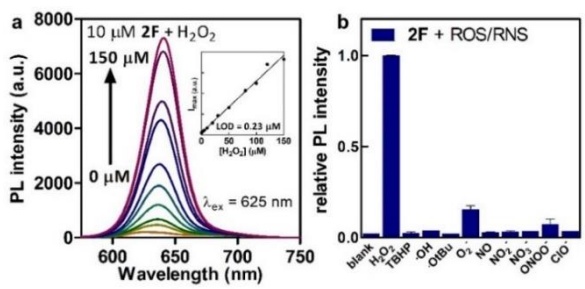

Figure 9. (a) Fluorescence spectra of 10 μM **2F** with increasing H_2O_2 concentrations in 1:1 (v/v) mixture of acetonitrile and potassium phosphate buffer (50 mM, pH 8.0) after 30 min incubation at 25℃. The inset shows the titration curve by the maximum intensities. (b) Normalized fluorescence intensities of **2F** at 640 nm with 200 μM of various ROS and RNS. The error bars represent the standard deviations of three measurements (λ_{ex} = 625 nm).

increasing amount of H_2O_2 added. The 61-fold increase in its ECL intensity proved that **2F** is a successful probe for H_2O_2. The ECL increase showed good linearity (R^2 = 0.9887) upon addition of H_2O_2 in the concentration range of 0 – 150 μM with a low detection limit of 0.51 μM.

To examine the specificity of **2F** toward H_2O_2, the maximum ECL intensities of **2F** were measured before and after the addition of ROSs/RNSs (reactive nitrogen species). The results, as shown in Figure 10b, indicate that **2F** selectively respond to H_2O_2. Among the interferents, only superoxide($\bullet O_2^-$) and peroxynitrite ($ONOO^-$) showed a little increase in the ECL intensity. The weak signal in response to superoxide is because of disproportionation which is known to generate H_2O_2.[45] Despite the reactivity of boronate ester toward peroxynitrite and hypochlorite (ClO^-),[46,47] peroxynitrite increased the ECL intensity only by 7.6% and hypochlorite

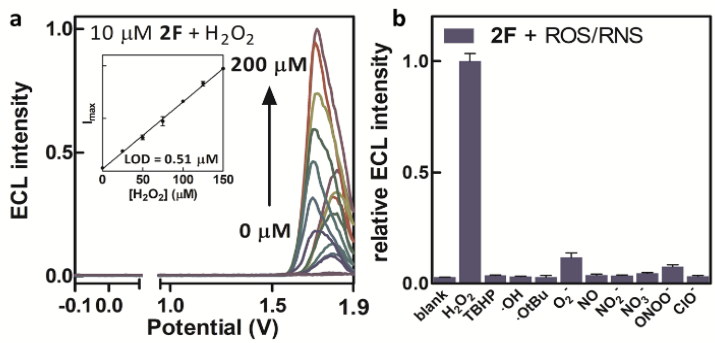

Figure 10. (a) Normalized ECL of probe **2F** after 30 min incubation with increasing H_2O_2 concentrations at 25℃ in a 1:1 (v/v) mixture of acetonitrile and potassium phosphate buffer (100 mM, pH 8.0). The inset shows a titration curve by the maximum intensity. (b) Normalized maximum ECL intensities of probe **2F** with various ROSs and RNSs after 30 min incubation at 25℃. The error bars represent the standard deviations of three measurements. 67.5 mM TPrA and 0.1 M tetrabutylammonium perchlorate (TBAP) were used as a coreactant and an electrolyte, respectively.

showed no response at all. No interference was observed upon the addition of the remaining ROSs/RNSs. Therefore, ECL probe **2F** has excellent selectivity along with high sensitivity toward H_2O_2.

B.2.5. Real Sample Detection

Thus far, we examined the performance of **2F** as an ECL probe in solution. As the analysis of biofluids such as blood and urine is a leading area in POCT, we wanted to quantify glucose in human serum by the standard addition method using enzymatic determination. It should be examined beforehand whether the presence of serum affected the reactivity or luminescence of the probe. The PL intensities of **2F** in presence and absence of serum indicate that diluted serum (×200) does not interfere with the analysis (Figure 11a). As some enzymes are denatured in certain solvent composition and GOx has its optimum pH at 5.5,[48] we compared the reaction rate of **2F** with either H_2O_2 or glucose/GOx to ensure that the enzyme works properly. Small delay was observed in generation of H_2O_2 in glucose/GOx but the

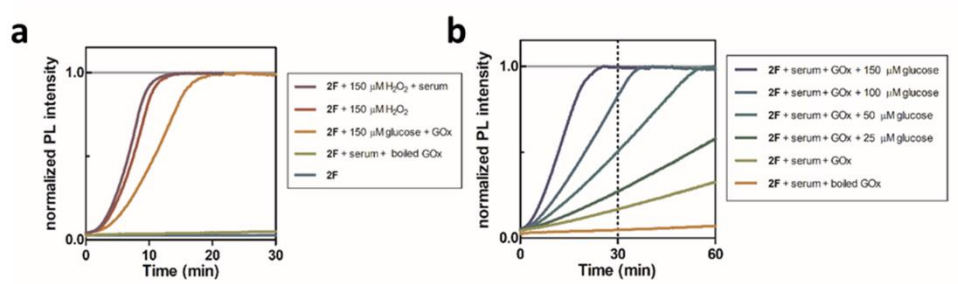

Figure 11. Normalized time-course measurements of the PL intensity at 640 nm of 10 μM probe **2F** when reacted with (a) 150 μM H_2O_2 + serum (×200), 150 μM H_2O_2, 150 μM glucose + 6.5 U/mL GOx, serum (×200) + boiled GOx (60°C, 1 h), none; (b) serum + boiled GOx, serum (×200) + 6.5 U/mL GOx + 0-150 μM glucose (λ_{ex} = 625 nm) in 1:1 (v/v) mixture of acetonitrile and potassium phosphate buffer (50 mM, pH 8.0) at 37°C.

measurements still could be done within 30 minutes (Figure 11a). A linear relationship was obtained between the PL intensity of **2F** (10 μM) and the increasing concentrations of glucose (0, 25, 50, and 100 μM) after 30 min incubation in diluted serum (×200) (Figure 11b).

The ECL intensity of probe **2F** was recorded upon addition of 0, 12.5, 25, 50, and 100 μM glucose after 30 min incubation with diluted serum (×200) and GOx. The standard addition curve was obtained showing a good linear relationship (R^2 = 0.9780) between the maximum ECL intensity and the amount of glucose added (Figure 12). The initial amount of glucose in the diluted serum was determined to be 21.79 μM, the -x value at the point of y= 0.04718, which is the maximum ECL intensity of probe **2F** when incubated with serum and denatured GOx by boiling at 60℃ for 1 h (Figure 11). By multiplying the dilution factor 200, the blood glucose

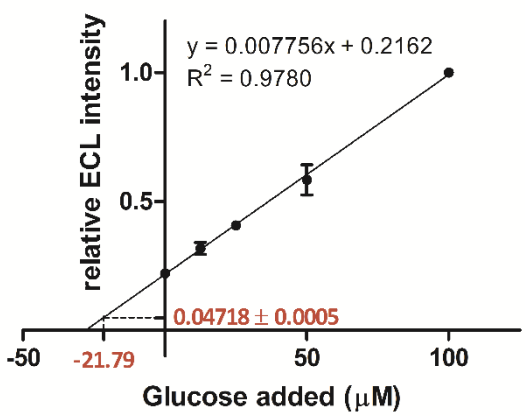

Figure 12. Determination of glucose in human serum by the standard addition method. The maximum ECL intensity of probe 10 μM **2F** was measured after 30 min incubation with serum (×200 dilution), GOx (6.5 U/mL), and glucose (0, 12.5, 25, 50, 100 μM) after 30 min incubation at 37℃ in 1:1 (v/v) mixture of acetonitrile and potassium phosphate buffer (50 mM, pH 8.0).

level of human serum was obtained as 4.36 mM, which is in well accordance with the normal plasma blood glucose levels (3.9–6.9 mM) for non-diabetics[49] and the result (4.81 mM ± 0.07) measured with a commercial glucose meter (One Touch Ultra, LifeScan). This quantitative analysis can be powerful evidence of the reliability and feasibility of **2F** into bedside testing.

B.3. Conclusion

In summary, three ECL H_2O_2 probes (**1**, **2**, **2F**) were designed and synthesized by combining pyridine-extended BODIPY fluorophores and benzyl boronate pinacol esters as a reaction site. **2F** was electrochemically stable during the ECL process by the full substitution on its BODIPY core and thus exhibited a selective 61-fold increase in the ECL intensity when exposed to H_2O_2. Moreover, fluorination on the reaction unit allowed ECL probe **2F** to detect H_2O_2 two-fold more rapidly compared to **2**. Furthermore, **2F** was successfully applied to the quantitative analysis of glucose in human serum by monitoring H_2O_2 released during the GOx reaction, proving the feasibility of **2F** for bioanalysis of real samples. To the best of our knowledge, this is the first report on BODIPY-based ECL probes for detection of H_2O_2 and determination of the blood glucose level in humans.

B.4. Experimental Section

Materials and Instruments

Unless otherwise mentioned, all materials were used as purchased from commercial suppliers including Sigma-Aldrich, TCI, and Acros without further purification. 2 mM stock solutions of probes in acetonitrile were prepared. 40 mM solution of H_2O_2 was made from 30 wt.% solution in water purchased in SAMCHUN chemicals. All the samples for the measurements were freshly prepared before the experiment. Fluorescent emission and UV-vis absorption spectra were measured in JASCO FP-8300 spectrofluorometer (JASCO, Tokyo, Japan) and V-730 spectrophotometer (JASCO, Tokyo, Japan), respectively. Thin layer chromatography (TLC) was performed on aluminum plates precoated with silica gel 60 F_{254} (Merck, Germany). Flash column chromatography was conducted with SilicaFlash® P60 (230-400 mesh) from SILICYCLE (Canada). ^{1}H and ^{13}C NMR spectra were obtained using Bruker Avance DPX-300 (Germany), Agilent 400-MR DD2 Magnetic Resonance System, and Varian 500 MHz NMR System.

Synthesis of B1

A mixture of benzoyl chloride (0.751 g, 5.34 mmol) and 2,4-dimethyl pyrrole (0.924 g, 9.71 mmol) in 50mL dichloromethane was stirred at room temperature for 3 h. Turning red, the reaction mixture was monitored by thin-layer chromatography (*n*-hexane: ethylacetate = 2:1). Once the reaction was completed, triethylamine (5 ml) and BF_3-Et_2O (5 ml) were added slowly at 0°C. After another 3 h stirring at room temperature, the resultant brown mixture was condensed via rotary evaporation and then washed with dichloromethane/water (×3). The organic layer was dried over sodium sulfate and concentrated. The crude product was purified by silica gel column chromatography (*n*-hexane ethyl acetate = 10:1) to afford orange powder (0.552 g, 1.70 mmol). Yield = 35%. ^{1}H NMR (400 MHz, $CDCl_3$) δ 7.49 – 7.41 (m, *J* = 1.8 Hz, 3H), 7.28 – 7.21 (m, 2H), 5.96 (s, 2H), 2.54 (s, 6H), 1.35 (s, 6H); ^{13}C NMR (100 MHz, $CDCl_3$) δ 155.39, 143.11, 141.69, 134.96, 131.38, 129.08, 128.89, 128.20, 127.90, 121.17, 14.55, 14.30.

Synthesis of B2

Compound **B2** was synthesized under the same reaction procedure for compound **B1** using 3-ethyl-2,4-dimethyl pyrrole (0.57 g. 4.06 mmol). Yield = 34% (0.476 g, 1.25 mmol) ^{1}H NMR (500 MHz, $CDCl_3$) δ 7.50 – 7.44 (m, 3H), 7.30 – 7.26 (m, 2H), 2.53 (s, 6H), 2.29 (q, *J* = 7.5 Hz, 4H), 1.27 (s, 6H), 0.98 (t, *J* = 7.5 Hz, 6H);. ^{13}C NMR (75 MHz, $CDCl_3$) δ 153.66, 140.23, 138.42, 135.80, 132.76, 130.80, 129.03, 128.77, 128.26, 17.08, 14.64, 12.50, 11.63.

Synthesis of py1

Compound **B1** (81 mg, 0.25 mmol) in dry DMF (5 ml) was mixed with 4- pyridine carboxaldehyde (108 mg, 1 mmol) and piperidine (188 mg, 1.7 mmol) in a 10 ml microwave tube. The tube was sealed and purged with N_2 for 15 min. The mixture was heated with stirring in a microwave oven at 100°C for 10 min. After the solvent was removed under low pressure, the purple crude was washed with ethyl acetate/brine (×3). The organic layer was dried over sodium sulfate and concentrated. Dark blue solid (20 mg, 0.052 mmol) was obtained by silica gel column chromatography (ethyl acetate: methanol = 10:1) and repeated recrystallization (dichloromethane/*n*-hexane). Yield = 21% ^{1}H NMR (500 MHz, $CDCl_3$) δ 8.65 (s, 4H), 7.90 (d, *J* = 16.3 Hz, 2H), 7.58 – 7.51 (m, 3H), 7.49 (d, *J* = 5.5 Hz, 4H), 7.37 – 7.31 (m, *J* = 7.1, 2.3 Hz, 2H), 7.26 (s, 2H), 7.16 (d, *J* = 16.3 Hz, 2H), 6.69 (s, 2H), 1.47 (s, 6H); ^{13}C NMR (75 MHz, $CDCl_3$) δ 153.79, 151.76, 149.70, 144.15, 143.38, 135.28, 134.50, 134.23, 133.08, 129.39, 128.00, 123.63, 121.51, 118.68, 14.72.; HRMS (FAB) m/z: $[M]^+$ calculated for $C_{31}H_{26}BF_2N_4$ 503.2219, observed 503.2224.

Synthesis of py2

Compound **py2** (51 mg, 91 μmol) was synthesized under the same reaction procedure for compound **py1** (95 mg, 0.25 μmol) using compound **2** instead. Yield = 40% (51 mg) ^{1}H NMR (400 MHz, $CDCl_3$) δ 8.63 (d, *J* = 5.7 Hz, 4H), 7.91 (d, *J* = 16.8 Hz, 2H), 7.55 – 7.48 (m, *J* = 2.3 Hz, 3H), 7.45 (d, *J* = 5.7 Hz, 4H), 7.34 – 7.28 (m, 2H), 7.14 (d, *J* = 16.8 Hz, 2H), 2.59 (q, *J* = 7.2 Hz, 4H), 1.33 (s, 6H), 1.15 (t, *J* = 7.5 Hz, 6H); ^{13}C NMR (100 MHz, $CDCl_3$) δ 149.90, 149.53, 144.61, 140.80, 140.12, 135.31, 134.76, 133.77, 132.79, 129.32, 129.25, 128.15,

124.09, 121.33, 18.24, 13.98, 11.55; HRMS (FAB) m/z: $[M]^+$ calculated for $C_{35}H_{34}BF_2N_4$ 559.2845, observed 559.2851.

Synthesis of probe 1

Compound **py1** (7 mg, 13.9 μmol) in acetonitrile (10 mL) was mixed with 4-bromomethyl phenyl boronic acid pinacol ester (9.1 mg, 30.6 μmol) with stirring. The reaction mixture was refluxed overnight and monitored by thin-layer chromatography (ethyl acetate). The mixture was cooled and evaporated when the reaction was completed. Green powder (11 mg, 10.0 μmol) was obtained by recrystallization (×3, dichloromethane/*n*-hexane). Yield = 72% ^{1}H NMR (300 MHz, $CDCl_3$) δ 9.21 (d, *J* = 5.5 Hz, 4H), 8.18 (d, *J* = 5.2 Hz, 4H), 7.95 (d, *J* = 16.2 Hz, 2H), 7.85 (d, *J* = 7.6 Hz, 4H), 7.63 (d, *J* = 3.7 Hz, 2H), 7.59 (d, 4H), 7.57 – 7.52 (m, *J* = 7.7 Hz, 5H), 6.99 (s, 2H), 6.12 (s, 4H), 1.45 (s, 6H), 1.34 (s, 24H); ^{13}C NMR (100 MHz, DMSO-d_6,$CDCl_3$) δ 152.26, 150.96, 150.72, 144.73, 144.66, 136.19, 135.73, 133.42, 129.89, 129.67, 129.49, 128.21, 127.90, 127.48, 125.07, 124.82, 120.84, 84.04, 65.59, 24.85, 15.29, 14.77; HRMS (FAB) m/z: $[M\text{-}2Br]^+$ calculated for $C_{57}H_{61}B_3F_2N_4O_4$ 936.4940, observed 936.4965

Synthesis of probe 2

The same method was applied for the synthesis of probe **2** using compound **py2** (10 mg, 35.8 μmol) instead of compound **py1**. Yield = 68 % (14 mg) ^{1}H NMR (500 MHz, $CDCl_3$) δ 9.51 – 9.40 (m, 4H), 8.23 (d, *J* = 6.3 Hz, 4H), 8.18 (s, 2H), 7.81 (d, *J* = 7.6 Hz, 4H), 7.63 (d, *J* = 7.9 Hz, 4H), 7.59 – 7.51 (m, *J* = 3.0 Hz, 5H), 7.35 (s, 2H), 7.33 – 7.29 (m, 4H), 5.99 (s, 4H), 2.62 (q, 4H), 1.35 (s, 6H), 1.30 (s, 24H), 1.12 (t, *J* = 7.3 Hz, 6H); ^{13}C NMR (125 MHz, $CDCl_3$) δ 152.82, 148.55, 148.36, 144.80, 141.24, 141.23, 137.30, 135.95, 135.67, 135.65, 129.73, 129.59, 128.58, 128.58, 127.81, 126.08, 125.03, 83.99, 63.78, 30.84, 24.83, 20.39, 13.95, 11.60; HRMS (FAB) m/z: $[M\text{-}2Br]^+$ calculated for $C_{61}H_{69}B_3F_2N_4O_4$ 992.5566, observed 992.5593

Synthesis of probe 2F

The same method was applied for the synthesis of **2** using compound **py2** (16.2 mg, 29 μmol) and 4-bromomethyl 2-fluorophenyl boronic acid pinacol ester (22.85 mg, 72.5 μmol) as starting materials. Yield = 57 % (19.6 mg) ^{1}H NMR (500 MHz, $CDCl_3$) δ 9.60 (d, 4H), 8.21 (d, *J* = 5.3 Hz, 4H), 8.16 (s, 2H), 7.78 – 7.73 (m, 2H), 7.55 (s, 4H), 7.52 (s, 2H), 7.35 (d, *J* = 10.8 Hz, 4H), 7.29 (d, *J* = 3.7 Hz, 2H), 6.07 (s, 4H), 2.60 (s, 4H), 1.34 (s, 6H), 1.30 (s, 24H), 1.13 – 1.09 (m, 6H); ^{13}C NMR (75 MHz, $CDCl_3$) δ 153.08, 152.36, 149.49, 148.28, 145.04, 141.33, 139.75, 138.39, 138.27, 137.32, 135.70, 134.46, 130.63, 129.65, 128.49, 127.76, 124.99, 124.67, 115.84, 84.10, 62.68, 29.71, 24.79, 18.26, 14.01, 11.64; HRMS (FAB) m/z: $[M-2Br]^+$ calculated for $C_{61}H_{67}B_3F_4N_4O_4$ 1028.5378, observed 1028.5404

Synthesis of M

The same method was applied for the synthesis of **2** using compound 4-methyl pyridine and 4-bromomethyl phenyl boronic acid pinacol ester as starting materials. Yield = 82% ^{1}H NMR (300 MHz, D_2O) δ 8.63 (d, *J* = 6.5 Hz, 2H), 8.63 (d, *J* = 6.5 Hz, 2H), 7.79 (d, *J* = 6.3 Hz, 2H), 7.74 (d, *J* = 7.9 Hz, 2H), 7.38 (d, *J* = 7.9 Hz, 2H), 5.66 (s, 2H), 2.55 (s, 3H), 1.12 (s, 12H).; ^{13}C NMR (100 MHz, DMSO-d_6) δ 159.93, 144.27, 137.97, 135.52, 129.83, 129.15, 128.55, 84.28, 62.57, 25.04, 21.90.; HRMS (FAB) m/z: $[M-Br]^+$ calculated for $C_{19}H_{25}BNO_2$ 310.1978, observed 310.1982.

Synthesis of MF

The same method was applied for the synthesis of **2** using compound 4-methyl pyridine and 4-bromomethyl 2-fluoro phenyl boronic acid pinacol ester as starting materials. Yield = 70% ^{1}H NMR (400 MHz, D_2O) δ 8.54 (d, *J* = 6.6 Hz, 2H), 7.73 (d, *J* = 6.4 Hz, 2H), 7.55 – 7.49 (m, 1H), 7.08 (d, *J* = 7.8 Hz, 1H), 6.99 (d, *J* = 10.2 Hz, 1H), 5.60 (s, 2H), 2.49 (s, 3H), 1.06 (s, 12H).; ^{13}C NMR (75 MHz, $CDCl_3$) δ 168.41, 165.10, 160.14, 144.40, 137.86, 129.24, 125.66, 124.82, 116.06, 84.27, 61.79, 25.03, 21.95.; HRMS (FAB) m/z: $[M-Br]^+$ calculated for $C_{19}H_{24}BFNO_2$ 328.1884, observed 328.1888.

pH dependence

50 mM of citrate/potassium phosphate buffer solutions of pH 5.0, 6.0, 7.0, 7.4, 7.8, 8.0, and 9.0 were prepared at 25℃. The total amount of sample in a quartz cuvette cell was 2.0 mL containing 10 μM probe and 200 μM H_2O_2 in 1:1 (v/v) mixture of acetonitrile and phosphate buffer. Maximum fluorescence intensity of sample was recorded for 2 h at excitation wavelength (λ_{ex}) of 610 nm for the probe **1** and 625 nm for **2** and **2F**.

Sensitivity and Selectivity

To a solution of 10 μM probe in 1:1 (v/v) mixture of acetonitrile and potassium phosphate buffer (50 mM, pH 8) were added aliquots of micromolar concentrations of H_2O_2 (0-200 μM). Fluorescence and UV-vis spectra of the sample were recorded after incubation at 25℃ until the probe reached 90 % conversion in response to 200 μM of H_2O_2. The limit of detection (LOD) was determined as three times the standard deviation of blank samples divided by the slope of the titration curve. The standard deviation of blank was obtained by at least 5 measurements of samples containing probe without an analyte. Maximum fluorescence intensity of probe was measured after reaction with 20 equivalence of reactive oxygen species (ROS) and reactive nitrogen species (RNS). ROS/RNS preparation are detailed in supporting information.

Real sample preparation

Human serum (from human male AB plasma, USA origin, sterile-filtered), GOx (from Aspergillus Niger), and D-(+)-glucose were purchased from sigma Aldrich and stored at -80℃ in small aliquots. The serum was deproteinized by centrifugation (13000 RPM, 2 minutes) after precipitation with acetonitrile. After acetonitrile is removed, the supernatant was diluted (×200) with a 1:1 (v/v) mixture of potassium phosphate buffer (50 mM, pH 8) and acetonitrile. 10 μM of probe, 6.5 U/mL of GOx, and 0-200 μM of D-(+)-glucose were added, and the mixture was incubated at 37℃ for 30 minutes.

ECL Experiments

ECL intensity was measured by an H-6780 photomultiplier tube (PMT) module (Hamamatsu Photonics K. K., Tokyo, Japan) which a home-made ECL cell was directly mounted on. All experimental conditions for PL were maintained for ECL experiments except adding 0.1 M tetrabutylammonium perchlorate (TBAP) as an electrolyte and using tri-*n*-propylamine (TPrA) pre-containing potassium phosphate buffer (100 mM, pH 8.0).

The Pt working electrode was polished with 0.05 mm alumina (Buehler, IL, USA) on a felt pad and sonicated in 1:1 (v/v) mixture of deionized water and absolute ethanol for 10 minutes. The electrode was fully dried with ultra-pure N_2 gas. All ECL experiments were simultaneously conducted with cyclic voltammetry (CV) by CH Instruments 650B Electrochemical Analyzer (CH Instruments, Inc., TX, USA) using a three-electrode setup. Pt was employed as working and counter electrodes and Ag/AgCl as reference electrode. Otherwise mentioned, every ECL signal was recorded in the potential range of -0.1 and 1.9 V at a scan rate of 1.0 V/s. All ECL data was the average of the first-scan values from three repeated experiments.

ROS/RNS preparation

tert-Butyl hydroperoxide (TBHP, 70% solution in water) was purchased from ACROS. Hydroxy radical (·OH) and *tert*-butoxy radical (·OtBu) were produced via the Fenton reaction. Superoxide ($O_2^{\cdot -}$) was generated from potassium superoxide (KO_2). Nitric oxide (NO) was generated from sodium nitroprusside (SNP) purchased from Fluka. Hypochlorite (ClO^-), nitrite (NO_2^-) and nitrate (NO_3^-) were produced from aqueous solutions of their sodium salts, respectively. Peroxynitrite ($ONOO^-$) was synthesized as follows: 0.6 M H_2O_2 was mixed with 0.6 M $NaNO_2$ at 0°C. 0.9 M NaOH was added right after the mixture was acidified with 0.7 M HCl. Remaining H_2O_2 was removed with manganese dioxide (MnO_2). The $ONOO^-$ concentration was determined by Beer-Lambert law ($\varepsilon = 1670\ cm^{-1}M^{-1}$ at 302 nm).

References and Notes

(1) Richter, M. M. *Chem. Rev.* **2004**, *104*, 3003.
(2) Gao, W.; Saqib, M.; Qi, L.; Zhang, W.; Xu, G. *Curr. Opin. Electrochem.* **2017**, *3*, 4.
(3) Miao, W. *Chem. Rev.* **2008**, *108*, 2506.
(4) Bard, A. J.; Debad, J. D.; Leland, J. K.; Sigal, G. B.; Wilbur, J. L.; Wohlsatdter, J. N.; Meyers, R.; Meyers, RA, Ed: 2000.
(5) Hu, L.; Xu, G. *Chem. Soc. Rev.* **2010**, *39*, 3275.
(6) Bader, J. M.; Kuwana, T. *J. Electroanal. Chem.* **1965**, *10*, 104.
(7) Santhanam, K. S. V.; Bard, A. J. *J. Am. Chem. Soc.* **1965**, *87*, 139.
(8) Liu, Z.; Qi, W.; Xu, G. *Chem. Soc. Rev.* **2015**, *44*, 3117.
(9) Rubinstein, I.; Bard, A. J. *J. Am. Chem. Soc.* **1981**, *103*, 512.
(10) Hesari, M.; Ding, Z. *J. Electrochem. Soc.* **2016**, *163*, H3116.
(11) Dini, D. *Chem. Mater.* **2005**, *17*, 1933.
(12) Jirka, G. P.; Martin, A. F.; Nieman, T. A. *Anal. Chim. Acta* **1993**, *284*, 345.
(13) Nepomnyashchii, A. B.; Bard, A. J. *Acc. Chem. Res.* **2012**, *45*, 1844.
(14) Li, H.; Sedgwick, A. C.; Li, M.; Blackburn, R. A. R.; Bull, S. D.; Arbault, S.; James, T. D.; Sojic, N. *Chem. Commun.* **2016**, *52*, 12845.
(15) Kim, K.-R.; Kim, H. J.; Hong, J.-I. *Anal. Chem.* **2019**, *91*, 1353.
(16) Maar, R. R.; Zhang, R.; Stephens, D. G.; Ding, Z.; Gilroy, J. B. *Angew. Chem.* **2019**, *131*, 1064.
(17) Chen, L.; Zeng, X.; Ferhan, A. R.; Chi, Y.; Kim, D.-H.; Chen, G. *Chem. Commun.* **2015**, *51*, 1035.
(18) Zinna, F.; Voci, S.; Arrico, L.; Brun, E.; Homberg, A.; Bouffier, L.; Funaioli, T.; Lacour, J.; Sojic, N.; Di Bari, L. *Angew. Chem.* **2019**.
(19) Bessette, A.; Hanan, G. S. *Chem. Soc. Rev.* **2014**, *43*, 3342.
(20) Loudet, A.; Burgess, K. *Chem. Rev.* **2007**, *107*, 4891.
(21) Lavis, L. D.; Raines, R. T. *ACS Chem. Biol.* **2008**, *3*, 142.
(22) Kowada, T.; Maeda, H.; Kikuchi, K. *Chem. Soc. Rev.* **2015**, *44*, 4953.
(23) Loudet, A.; Burgess, K. *Chem. Rev.* **2007**, *107*, 4891.
(24) Chang, M. C.; Pralle, A.; Isacoff, E. Y.; Chang, C. J. *J. Am. Chem. Soc.* **2004**, *126*, 15392.
(25) Abo, M.; Urano, Y.; Hanaoka, K.; Terai, T.; Komatsu, T.; Nagano, T. *J. Am. Chem. Soc.* **2011**, *133*, 10629.
(26) Shin, I.-S.; Bae, S. W.; Kim, H.; Hong, J.-I. *Anal. Chem.* **2010**, *82*, 8259.
(27) Veal, E. A.; Day, A. M.; Morgan, B. A. *Mol. Cell* **2007**, *26*, 1.

(28) Rhee, S. G. *Science* **2006**, *312*, 1882.
(29) Guo, R.; Wang, Y.; Yu, S.; Zhu, W.; Zheng, F.; Liu, W.; Zhang, D.; Wang, J. *RSC Adv.* **2016**, *6*, 59939.
(30) Wilson, R.; Turner, A. P. F. *Biosens. Bioelectron.* **1992**, *7*, 165.
(31) Monnier, L.; Mas, E.; Ginet, C.; Michel, F.; Villon, L.; Cristol, J.-P.; Colette, C. *Jama.* **2006**, *295*, 1681.
(32) Giugliano, D.; Ceriello, A.; Esposito, K. *Am. J. Clin. Nutr.* **2008**, *87*, 217S.
(33) Boden, G.; Sargrad, K.; Homko, C.; Mozzoli, M.; Stein, T. P. *Ann. Intern. Med.* **2005**, *142*, 403.
(34) Lippert, A. R.; Van de Bittner, G. C.; Chang, C. J. *Acc. Chem. Res.* **2011**, *44*, 793.
(35) Miller, E. W.; Albers, A. E.; Pralle, A.; Isacoff, E. Y.; Chang, C. J. *J. Am. Chem. Soc.* **2005**, *127*, 16652.
(36) Kuivila, H. G.; Armour, A. G. *J. Am. Chem. Soc.* **1957**, *79*, 5659.
(37) Wang, J.; Zhu, W.; Niu, G.; Jiang, G.; Chen, Q.; Gao, P.; Li, Y.; Zhang, G.; Fan, X.; Tang, B. Z. *Chem. Commun.* **2018**, *54*, 13957.
(38) Neupane, L. N.; Lohani, C. R.; Kim, J.; Lee, K.-H. *Tetrahedron* **2013**, *69*, 11057.
(39) Hou, J.; Qian, M.; Zhao, H.; Li, Y.; Liao, Y.; Han, G.; Xu, Z.; Wang, F.; Song, Y.; Liu, Y. *Anal. Chim. Acta* **2018**, *1024*, 169.
(40) Van de Bittner, G. C.; Dubikovskaya, E. A.; Bertozzi, C. R.; Chang, C. J. *Proc. Natl. Acad. Sci.* **2010**, *107*, 21316.
(41) Xu, J.; Li, Q.; Yue, Y.; Guo, Y.; Shao, S. *Biosens. Bioelectron.* **2014**, *56*, 58.
(42) Cao, S.; Christiansen, R.; Peng, X. *Chem. - Eur. J.* **2013**, *19*, 9050.
(43) Alouane, A.; Labruere, R.; Le Saux, T.; Schmidt, F.; Jullien, L. *Angew. Chem., Int. Ed.* **2015**, *54*, 7492.
(44) Roy, K.; Popelier, P. L. *J. Phys. Org. Chem.* **2009**, *22*, 186.
(45) Bielski, B. H. J.; Allen, A. O. *J. Phys. Chem.* **1977**, *81*, 1048.
(46) Jiao, X.; Li, Y.; Niu, J.; Xie, X.; Wang, X.; Tang, B. *Anal. Chem.* **2017**, *90*, 533.
(47) Wang, S.; Chen, L.; Jangili, P.; Sharma, A.; Li, W.; Hou, J.-T.; Qin, C.; Yoon, J.; Kim, J. S. *Coord. Chem. Rev.* **2018**, *374*, 36.
(48) Tsuge, H.; Natsuaki, O.; Ohashi, K. *J. Biochem.* **1975**, *78*, 835.
(49) Ma, J.-L.; Yin, B.-C.; Wu, X.; Ye, B.-C. *Anal. Chem.* **2017**, *89*, 1323.

국문초록

전기화학발광은 현장진단으로 활용될 수 있는 강력한 분석법이다. 지금까지 BODIPY 를 기반으로 한 유기 전기화학발광체에 대한 보고가 많이 이루어졌지만, 이를 이용한 분자검출에 대한 연구는 거의 이루어지지 않았다. 본 연구에서는 활성산소종 중 하나인 과산화수소 BODIPY 프로브를 개발하여 당뇨 등의 질병 진단에 필수인 글루코오스 검출을 시행하였다. 프로브의 원활한 전기화학발광을 위해 알킬기를 도입해 라디칼 안정성을 높이고 반응기 옆에 불소 음이온을 도입함으로써 과산화수소 검출 속도를 향상시켰다. 결과적으로 개발된 BODIPY 전기화학발광 프로브는 높은 감도와 선택성, 빠른 검출 속도를 보였으며, 실제 혈청 샘플 내의 글루코오스 농도를 정량하는 추가 실험을 통해 현장진단으로의 높은 활용 가능성을 증명하였다.

주요어: 전기화학발광프로브, BODIPY, 과산화수소, 글루코오스, 혈당 수치 검출, 글루코오스 산화효소

학번: 2017 - 21746